Determination of Crop Coefficients for Flood-Irrigated Winter Wheat in Southern New Mexico Using Three Contrasting ETo Estimation Methods

Hui Yang * , Manoj K. Shukla , Adam Gonzalez , Yusen Yuan

Posted Date: 9 July 2024

doi: 10.20944/preprints202407.0673.v1

Keywords: winter wheat; ETo estimation method; crop coefficient

Article

Determination of Crop Coefficients for Flood-Irrigated Winter Wheat in Southern New Mexico Using Three Contrasting ETo Estimation Methods

Hui Yang *, Manoj K. Shukla, Adam Gonzalez and Yusen Yuan

Plant and Environmental Sciences Department, New Mexico State University, Las Cruces, NM 88003, USA
* Correspondence: yangh@nmsu.edu; Tel.: +1-575-571-3983

Abstract: Crop coefficient (K_c), the ratio of crop evapotranspiration (ET_c) to reference evapotranspiration (ET_o), is used to schedule an efficient irrigation regime. This research was conducted to investigate variations of ET_c and growth-stage-specific K_c in a flood-irrigated winter wheat as a forage crop from 2021 to 2023 in the Lower Rio Grande Valley of southern New Mexico, USA, and evaluate the performances of the two temperature-based ET_o estimation methods of Hargreaves-Samani and Blaney-Criddle with the widely used Penman-Monteith method. Results indicated that the total ET_c over the whole growth stage for flood-irrigated winter wheat was 556.4 mm on a two-year average, while the average deep percolation (DP) was 2.93 cm and 2.77 cm, accounting for 28.8% and 27.2% of applied irrigation water, respectively in the 2021-22 and 2022-23 growing seasons. The ET_o over the growing season computed by Penman-Monteith, Hargreaves-Samani, and Blaney-Criddle equations were 867.0 mm, 1015.0 mm, and 856.2 mm in 2021-22, and 785.6 mm, 947.0 mm, and 800.1 mm in 2022-23, respectively. The Hargreaves-Samani method performed better than the Blaney-Criddle method with higher statistical indicators of model efficiency coefficient (CE), and smaller mean bias error (MBE), mean absolute error (MAE), and the root mean square error (RMSE) in both growing seasons. The result of a global sensitivity analysis showed that the mean temperature is main driving factor for estimated ET_o based on Blaney-Criddle and Hargreaves-Samani, but the sensitivity percentage for Blaney-Criddle was 76.9%, which was much higher than that of 48.9% for Hargreaves-Samani, given that Blaney-Criddle method is less accurate in ET_o estimation for this area especially during the hottest season from May to August. In contrast, wind speed and maximum temperature were the main driving factors for the Penman-Monteith method, with sensitivity percentages of 70.9% and 21.9%, respectively. The two-year average crop coefficient (K_c) values at the initial, mid, and late growth stage were 0.54, 1.1, and 0.54 based on Penman-Monteith, 0.51, 1.0 and 0.46 based on Blaney-Criddle, and 0.52, 1.2 and 0.56 based on Hargreaves-Samani. Results showed that the Hargreaves-Samani equation serves as an alternative tool to predict ET_o when fewer meteorological variables are available. The calculated local growth-stage-specific K_c can help improve irrigation water management in this region.

Keywords: winter wheat; ET_o estimation method; crop coefficient

1. Introduction

Wheat is the main cereal crop to supply essential food for the world population and winter wheat contributes approximately 80% of global wheat production [1]. The United States of America (USA) is a major producer and the third-largest wheat exporter worldwide [2]. Winter wheat (Triticum aestivum L.) is commonly grown in the southern Great Plains of the USA, including Oklahoma, Kansas, New Mexico, and Texas as a dual-purpose crop for grain and forage production

 doi:10.20944/preprints202407.0673.v1

[3]. The winter wheat production for 2020 in the USA totaled 31.8 million tons, of which production in New Mexico was estimated at 87.6 thousand tons, a decrease of 2% compared to 2019 [4]. According to the 2022 report of crop progress and condition in New Mexico, 84% of the winter wheat harvested for grain was in a very poor or poor condition across a limited area, compared with 57% in 2021 while the 5-year average was 33% [5]. The water scarcity in the drier areas of western US, especially the increasing water shortage in irrigated agriculture is the main reason causing the reduction of yield. Although planting strategies and yield of different winter wheat cultivars have been documented in the Southeast and Great Plains of the USA [6,7], detailed information on winter wheat water use (evapotranspiration) and crop coefficient is still lacking, which is required for managing crop water demands for Lower Rio Grande Valley in New Mexico. In this region, Harkey (coarse-silty, mixed, calcareous, thermic Typic Torrifluvents) - Glendale (fine-silty, mixed, calcareous, thermic Typic Torrifluvents) soil is prevalent [8] and the climate is arid continental [9]. New Mexico Interstate Stream Commission (NMISC) has completed and accepted the Lower Rio Grande Regional Water Plan to meet regional water needs for the next 40 years since 2003 [9].

Irrigation is required for maintaining cereal production in arid- and semi-arid regions. The actual evapotranspiration (ET_c) is a key parameter in estimating water requirements for efficient irrigation. To date, many methods of ET_c measurements have been established directly or indirectly using lysimeters [10], eddy covariance [11], Bowen-ratio energy balance [12], soil water balance [13], sap flow coupled with micro-lysimeters [14], and remote sensing energy balance [15] or satellite-based ET_c with vegetation indices [16]. Numerous mathematical models have been developed to estimate ET_c, as the product of the specific crop coefficient (K_c) and reference evapotranspiration (ET_o) [17–19]. Generally, the tabulated K_c values provided by Allen et al. [20] were used in ET_c estimation for different locations and seasons; however, the adjusted K_c based on local conditions could further meet the need for precise irrigation scheduling [21]. To the best of our knowledge, no previous studies have investigated variations of ET_c and local K_c for flood-irrigated winter wheat in southern New Mexico, which in turn affect the accuracy of irrigation amount supplied on demand throughout the crop growing season in this region.

Among mathematical equations for obtaining ET_o, the Penman-Monteith method has been reported to be very precise under different environmental conditions [16,22–24]. However, the application of the Penman-Monteith equation requires several meteorological variables, which are often not available [25–27]. Alternatively, the application of simple temperature-based equations is used for ET_o estimation at the local scale. Notably, air temperature is the earliest monitored meteorological variable among the inputs of ET_o computation and it has been reported that the changes in temperature and solar radiation resulted in at least 80% of ET_o variability [28]. The available temperature-based equations include the well-known Hargreaves-Samani [29] and Blaney-Criddle equations [30]. The Blaney-Criddle was first developed for New Mexico in 1942 to calculate consumptive water use for limited crops, such as alfalfa, cotton as well as deciduous trees in NM Pecos River Valley [31,32]. The Hargreaves-Samani equation was recommended as accurate and simple in several studies [33,34]. Some studies calibrated and validated both equations under diverse local conditions; however, the applications of the two equations have yielded contrasting conclusions in different studies, as both equations could under- or over-estimate ET_o for a specific crop under a certain climate [35,36]. To our knowledge, no prior studies have applied these two equations for ET_o estimation in the Lower Rio Grande Valley of southern New Mexico. Therefore, the specific objectives of this study were to 1) evaluate the performances of temperature-based equations of Hargreaves-Samani and Blaney-Criddle in the Lower Rio Grande Valley of southern New Mexico comparing their outputs with those from the Penman-Monteith method, 2) determine the influences of the meteorological variables on simulated ET_o using global sensitivity analysis for all three ET_o estimation approaches, 3) estimate crop evapotranspiration for flood irrigated winter wheat with forage purpose using the water balance method, and 4) investigate local crop coefficient (K_c) of winter wheat for the study area.

 doi:10.20944/preprints202407.0673.v1

2. Materials and Methods

2.1. Experimental Site

This study was conducted at the Leyendecker Plant Science Research Center (Latitude 32°12.326'N, Longitude 106°44.781'W at an altitude of 1174 m above sea level) of New Mexico State University, located 14.5 km south of Las Cruces from 2021-2023. The experimental site is 1.2 acres in size, winter wheat seeds (Weathermaster, supplied by West Gaines Seed, Inc.) were sown on September 29th, 2021 and September 30th, 2022, harvested on May 20th, 2022, and May 22nd, 2023, respectively. The seeds were planted using a plot drill (John Deere 450, Grand Detour, IL) at a seeding rate of 70 lbs/acre with a drill spacing of 0.15 m for both years. The preharvest plant height was 92.3±1.2 cm and 81.6±0.8 cm for the 2021-22 and 2022-23 seasons, respectively. The physical properties of the soil in the study area are given in Table 1. Soil at the experimental site is classified as Glendale, the typical surface for Glendale soil is clay and the layers below are clay loam and very fine sand [8]. The soil has low hydraulic conductivity for root zone layers. The average bulk density, water content at field capacity, and wilting points are 1.34 g cm^{-3}, 0.37 cm^3 cm^{-3}, and 0.21 cm^3 cm^{-3}, respectively (Table 1). Chemical analysis of soil and irrigation water is given in Table 2. The electrical conductivity for layers 40-60 and 60-80 cm is much higher than the other layers, which is consistent with the concentrations of sodium and chloride (Table 2). The crop was flood-irrigated with well water. A total of 8 and 7 irrigation events were applied throughout the 2021-22 and 2022-23 growing seasons, respectively according to the local farm practices. A flow meter was installed at the outlet of the pump to measure the irrigation flow rate and volume, the pump pushes 2500 gallons of water per minute and each irrigation event lasts 45 minutes. The irrigation interval was about 30 days for the first three irrigations from the beginning of the growing season until mid-November, after that, it was once every 20 days from February until late May. The crop received 101.6 mm during each irrigation event with a total of 812.8 and 711.2 mm during the growing seasons of 2021-22, and 2022-23, respectively. The observed groundwater table at the Rio Grande riverbed is 3.34 m during the winter of 2021.

Table 1. Soil particle size distribution and textural class at random 4 locations, soil physical properties at random 3 locations covering the whole experimental winter wheat plot on Leyendecker farm, Las Cruces, NM. The data are average values + standard error of three replicates.

Depth (cm)	Particle Size Distribution (%)			Texture
	Sand	Silt	Clay	
0-20	24.0±0.6	23.0±0.5	53.0±0.4	clay
20-40	32.3±0.9	16.2±0.7	51.5±0.6	clay
40-60	17.8±0.9	20.4±0.9	61.8±0.3	clay
60-80	30.3±1.3	40.1±1.0	29.6±1.4	clay loam
80-100	58.4±2.0	23.7±1.5	17.9±1.4	sandy loam
Depth (cm)	BD	K_s	FC	WP
0-15	1.34±0.16	0.066±0.17	0.38±0.05	0.21±0.04
15-30	1.35±0.16	0.066±0.17	0.38±0.05	0.21±0.05
30-50	1.39±0.15	0.001±0.00	0.39±0.04	0.23±0.00
50-80	1.29±0.16	0.255±0.33	0.34±0.10	0.17±0.11

BD=bulk density (g cm^{-3}), K_s=saturated hydraulic conductivity (cm h^{-1}), FC=soil water content at field capacity at 30 kPa (cm^3 cm^{-3}), and WP=soil water content at wilting point at 1500 kPa (cm^3 cm^{-3}).

 doi:10.20944/preprints202407.0673.v1

2.2. Measurements and Data Collection

2.2.1. Soil Physical Properties

Soil samples from the experimental plot were collected at five depths (0-20 cm, 20-40 cm, 40-60 cm, 60-80 cm, and 80-100 cm) from 4 locations to determine the soil texture in 2021. The depth-wise samples were analyzed separately for each location. The percentage of clay, silt, and sand in each sample was determined in the laboratory by the hydrometer method [37]. Soil textures were identified based on the USDA textural triangle. Soil bulk density was determined by the core method [38]. Individual soil cores (5 cm diameter and 5 cm height) were partitioned into depth intervals of 0-15 cm, 15-30 cm, 30-50 cm, and 50-80 cm at three locations. Saturated hydraulic conductivity was determined by the constant head method [39], and soil water retention by the pressure chamber method [40]. The volumetric water content at 30 kPa and 1500 kPa was defined as field capacity and wilting point water content, respectively. The chemical analysis of soil and irrigation water was tested in Ward Laboratories, Inc. (Nebraska, USA).

Table 2. Chemical properties of pre-tilling soil at 5 different depths within winter wheat plot as well as irrigation water chemical properties during the winter wheat growing season. The data are average values + standard error of three replicates.

Properties	Unit	Soil					Irrigation water
		0-20 cm	20-40 cm	40-60 cm	60-80 cm	80-100 cm	
pH		8.13±0.03	8.13±0.09	7.93±0.09	8.03±0.03	8.20±0.26	7.73±0.40
Electrical conductivity	dS/m	1.67±0.32	1.84±0.54	3.46±0.23	2.74±0.92	1.84±0.70	1.01±0.11
Sodium	ppm	518.3±127.6	719.7±200.9	1071.7±354.8	940.0±41	454.7±120.6	96.3±15.4
Chloride	ppm	121.9±13.5	108.4±33.1	142.6±61.2	190.3±76.6	111.6±57.8	93.5±2.40
Calcium	ppm	5581.0±32.5	5482.0±52.2	6952.7±511.0	5685.7±905.0	3865.0±1468.8	95.8±21.3
Magnesium	ppm	578.3±10.1	639.7±23.0	795.7±60.6	567.7±134.2	360.0±128.5	18.5±2.02
Potassium	ppm	430.0±38.2	407.3±23.7	381.3±44.5	198.7±42.0	171.0±80.6	6.25±0.25
Nitrate	ppm	31.4±9.7	10.83±2.04	7.63±2.40	4.47±1.73	4.33±1.87	34.1±18.5
Sulfur	ppm	219.6±61.7	236.0±76.5	1156.4±240.6	1347.1±601.7	630.7±279.4	70.8±3.38

2.2.2. Soil Water Content

At the center of the experimental site, 4 Teros 12 sensors (METER Group, Pullman, WA) were installed horizontally at the depths of 15, 30, 50 and 80 cm to continuously monitor the diurnal volumetric soil water content. According to the particle size distribution for 0-100 cm soil depths of 4 locations covering the whole plot, the soil variability through the profile (CV =7.14% for clay; CV= 11.3% for sand on five-layer average) within the plot is small, we decided to place one set of soil moisture sensors at the center of the plot. A second set of sensors at the same depths was installed about 3.5 m from the first location and the difference in soil moisture content was low (the average CV=1.60%, 4.55%, 5.62%, and 3.16% for soil depths of 15, 30, 50 and 80 cm, respectively in one

 doi:10.20944/preprints202407.0673.v1

irrigation cycle). All sensor data were automatically broadcast on Lora frequencies across different channels using ebyte22 hardware. A linear equation was suggested by the Meter group in the manual for the calibration of mineral soil types with saturated paste extract EC_s ranging from 0 dS/m to 8 dS/m. Volumetric water content is calculated using the following equation:

$$\theta = C_0 \times RAW + C_1 \quad (1)$$

where θ is the volumetric water content (cm^3 cm^{-3}); RAW is the raw sensor output, C_0, C_1 are the calibration coefficients (C_0=3.879×10-4, C_1=-0.6956).

Soil-specific calibration equations usually perform better than the manufacturer's [41], concurrently, all of the devices required separate calibrations for different soil horizons [42]. In our study, the gravimetric method was used to calibrate the measured volumetric water content data by Teros 12 sensors. Undisturbed and loose soil samples were collected at the depths of 15, 30, 50, and 80 cm from 4 locations near the Teros 12 sensors at two-to-five-day intervals during the period from Feb 16th to May 20th. Thus, the sample size used in the calibration was 52. After that, soil samples were weighed and oven-dried at 105 ℃ until constant weight. The calibration was performed for 4 different soil horizons respectively at 15, 30, 50, and 80 cm. The new coefficients C_0 and C_1 for Eq. (1) were derived for each sensor depth, and the calibration Eq. (1) was fitted using the nonlinear least-squares approach. The estimated coefficients C_0 and C_1 for the Eq. 1 at 15, 30, 50, and 80 cm sensor depths are shown in Table 3.

Table 3. Estimated coefficients C_0 and C_1 for the calibration of Teros 12 sensors (Eq. 1) at each soil depth of 15, 30, 50, and 80 cm.

Sensor depths (cm)	New coefficients for calibration Eq. 1		R^{2*}
	C_0	C_1	
15	3.771×10^{-4}	-0.6677	0.916
30	3.558×10^{-4}	-0.6065	0.867
50	3.503×10^{-4}	-0.5929	0.817
80	3.700×10^{-4}	-0.6551	0.769

* Coefficient of determination of volumetric water contents measured by Teros 12 sensors using new calibration versus volumetric water contents converted by the measurements with the gravimetric method.

The Teros 12 determined volumetric water contents were recalculated from measured raw data and the estimated coefficients using Eq. 1. The coefficients of determination (R^2) between the modified volumetric water contents and the gravimetrically determined volumetric water contents were always greater than 0.80 at the depths of 15, 30, 50 cm, while at 80-100 cm depth R^2 was 0.77 (Figure 1 and Table 3).

 doi:10.20944/preprints202407.0673.v1

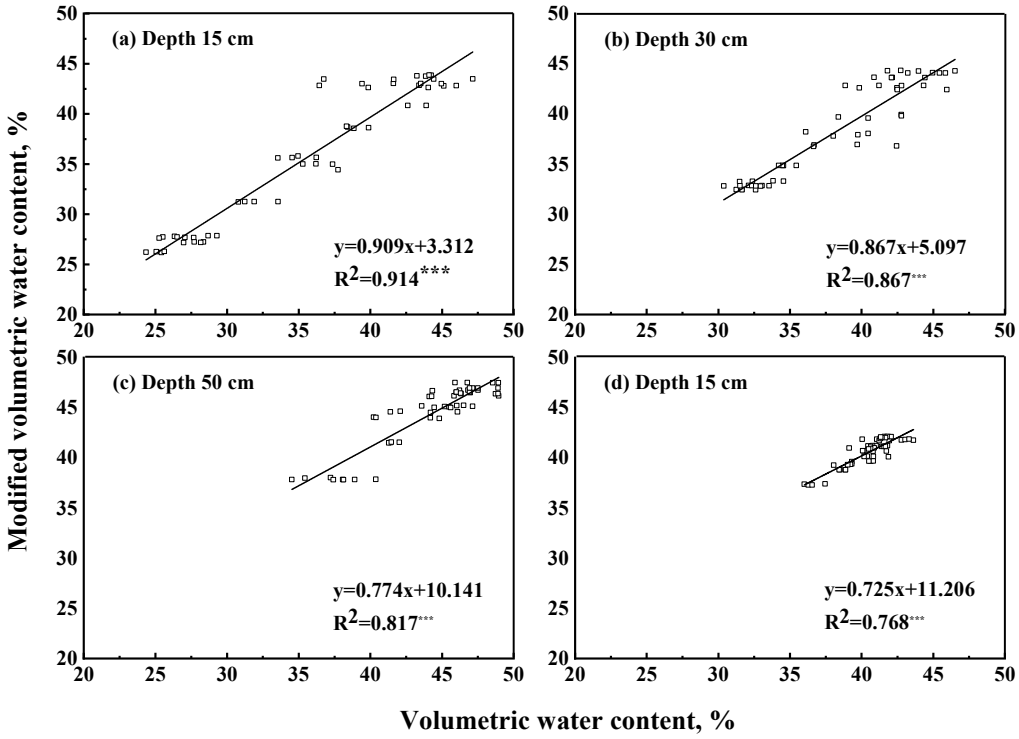

Figure 1. Relationships between volumetric soil water contents converted from the measured gravimetric water contents and the modified volumetric water contents measured by Teros 12 sensors using new calibration coefficients at 15 cm (a), 30 cm (b), 50 cm (c), and 80 cm (d) soil depths.

2.2.3. Meteorology

The climate of the experimental area is classified as semi-arid with an annual precipitation of 203-255 mm and an average annual temperature of 16-24℃ [9]. An ATMOS-41 weather station was installed 300 m northwest of the experimental site to record daily precipitation, air temperature, relative humidity, wind speed, and solar radiation at 15-minute intervals. The average daily relative humidity (RH), vapor pressure deficit (VPD), air temperature (T_a) and solar radiation (R_s) over the two growing periods of winter wheat were 48.2±1.1% and 52.6±1.1%, 1.02±0.04 kPa and 0.83±0.03 kPa, 11.3±0.4 ℃ and 10.8±0.4 ℃, 188.3±4.4 W/m² and 174.6±4.6 W/m², respectively (Figure 2).

 doi:10.20944/preprints202407.0673.v1

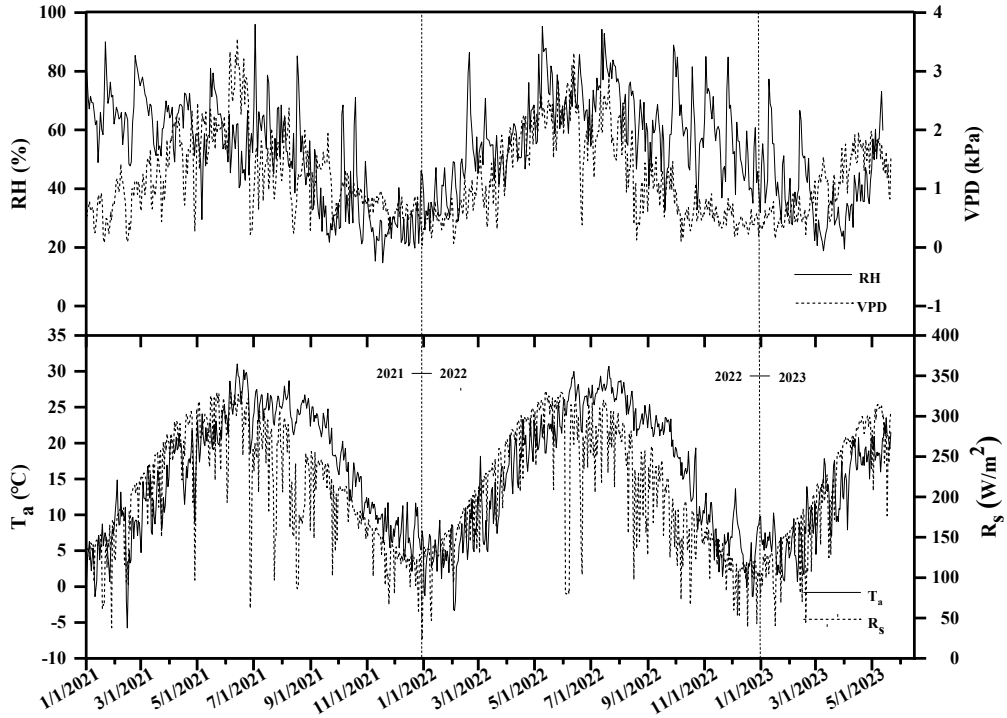

Figure 2. The microclimate condition of daily relative humidity (RH, %) and vapor pressure deficit (VPD, kPa) (a), air temperature (T_a, ℃) and solar radiation (R_s, W/m^2) (b) during the 2021-22 and 2022-23 growth seasons of winter wheat at the Leyendecker Plant Science Research Center, Las Cruces, NM, USA.

2.3. Crop Coefficients Approach

Crop coefficient K_c is defined as the ratio of crop evapotranspiration (ET_c)to reference evapotranspiration (ET_o), it varies throughout the crop growth stage with the surface resistance and aerodynamic of the crop and reference crop [17]. Generally, K_c is calculated by single or dual approaches in FAO56, the derivation of K_c is consistent with the growth change of the crop such as height, leaf area, and albedo of the crop-soil surface [17]. However, we chose to calculate K_c as the ratio of ET_c to ET_o because we had an estimate of ET_c using the water balance method. Several previous studies have also estimated K_c using water balance [43–45]:

$$k_c = ET_c / ET_o \quad (2)$$

The average daily ET_c was estimated by the water balance equation [46]:

$$ET_c = \left[\frac{(I + P - DP + \sum_{i=1}^{n} (\theta_1 - \theta_2)\Delta S_i}{\Delta t} \right] \quad (3)$$

Where I is irrigation depth (mm), P is precipitation (mm), DP is deep percolation below the upper 80 cm soil depth (mm), ΔS is the thickness of each soil layer (mm), which are 150, 150, 200, and 300 mm in this study, θ_1 and θ_2 are the volumetric soil water content at times one and two (%), and Δt is the time interval between two consecutive irrigation events in days. In this study, the surface runoff is 0, and capillary rise from the groundwater table is 0 since the groundwater table is below 3 m and the soil in the deeper layer is sandy.

Deep percolation (DP, cm) was calculated using the method proposed by Doorenbos and Pruitt [30] expressed as:

 doi:10.20944/preprints202407.0673.v1

$$DP = \begin{Bmatrix} 0 & if \quad SWC < SWC_{FC} \\ SWC - SWC_{FC} & if \quad SWC > SWC_{FC} \end{Bmatrix} \tag{4}$$

where SWC is the in-situ soil water stored in the root zone (cm), and SWC_{FC} is the soil water stored at field water holding capacity for the same depth (cm). DP was calculated using soil water content and field water holding capacity data for the depths of 15, 30, 50 and 80 cm.

Methods of reference evapotranspiration estimation

Selecting a proper method of computing reference evapotranspiration depends on the type, quality and length of the available climatic data.

The Penman-Monteith method is recommended when temperature, humidity, wind speed, and solar radiation data are available because of its accuracy for any environment. It is obtained by the following equation [47]:

$$ET_o = \frac{\left[0.418\Delta(R_n - G) + \gamma \frac{900}{T+273} u_2 (e_s - e_a)\right]}{\Delta + \gamma(1 + 0.34u_2)} \tag{5}$$

where R_n is the net radiation at crop surface (MJ m^{-2} day^{-1}), G the soil heat flux density (MJ m^{-2} day^{-1}), Δ the slope of the vapor pressure curve (kPa $℃^{-1}$), γ the psychrometric constant (kPa $℃^{-1}$), T the mean daily air temperature at 2 m height (℃), e_s-e_a the saturation vapor pressure deficit (kPa), u_2 the wind speed at 2 m height (m s^{-1}). The computation of all parameters required for the ET_o calculation followed the method of Allen et al. [20].

The temperature-based Blaney-Criddle method for estimating ET_o has been widely used in the western USA as described by Doorenbos and Pruitt [30]. This method can be commonly described by [48]:

$$ET_o = c_e(a_t + b_t pT) \tag{6}$$

The unit of ET_o in this equation is inch/d, T is the mean air temperature for the period (°F), p is the mean daily percent of annual daytime hours, and a_t and b_t are adjustment factors based on the climate of this region, c_e is the adjustment factor based on the elevation above sea level. The calculations of the three factors are given as:

$$c_e = 0.01 + 3.049 \times 10^{-7} E_{lev} \tag{7}$$

$$a_t = 3.937\left(0.0043RH_{\min} - \frac{n}{N} - 1.41\right) \tag{8}$$

$$b_t = b_n + b_u \tag{9}$$

$$b_n = 0.82 - 0.0041RH_{\min} + 1.07\frac{n}{N} - 0.006RH_{\min}\frac{n}{N} \tag{10}$$

$$b_u = (1.23U_d - 0.0112RH_{\min}U_d)/1000 \tag{11}$$

where E_{lev} is the elevation above sea level (ft), RH_{min} the mean daily minimum relative humidity (%), n/N the ratio of actual to possible sunshine hours, U_d the mean daytime wind speed at 2 meters above the ground (mi/d).

Another temperature-based method was defined by Hargreaves and Samani [29]:

$$ET_o = 0.0023 \times 0.408R_a(T_{mean} + 17.8)(T_{\max} - T_{\min})^{0.5} \tag{12}$$

where R_a is the extraterrestrial radiation (MJ m^{-2} d^{-1}) obtained from a set of equations [34], T_{mean}, T_{max} and T_{min} are mean, maximum, and minimum air temperature during the calculation period (℃).

 doi:10.20944/preprints202407.0673.v1

Growing degree days (GDD, ℃ day) were computed as follows [49]:

$$GDD_i = T_{avg} - T_b \tag{13}$$

GDD_i is the growing degree days for day i (℃day), if $T_{avg} < T_b$, GDD=0, T_{avg} is the daily mean temperature (℃), T_b is the crop-specific base air temperature taken as 0 ℃ for winter wheat [50].

Statistical Indicators

The statistical indicators used to evaluate the performance of the methodologies against the reference evapotranspiration computed by the Penman-Monteith method were the Nash-Sutcliffe model efficiency coefficient (CE), the mean bias error (MBE), the mean absolute error (MAE), and the root mean square error (RMSE):

$$CE = 1 - \frac{\sum_{i=1}^{n}(ET_i - ET_{PMi})^2}{\sum_{i=1}^{n}(\overline{ET_{PMi}} - ET_i)^2} \tag{14}$$

$$MBE = \frac{1}{n}\sum_{i=1}^{n}(ET_i - ET_{PMi}) \tag{15}$$

$$MAE = \frac{1}{n}\sum_{i=1}^{n}\left|ET_i - ET_{PMi}\right| \tag{16}$$

$$RMSE = \left[\frac{1}{n}\sum_{i=1}^{n}(ET_i - ET_{PMi})^2\right]^{0.5} \tag{17}$$

where ET_{PM} and ET_i are the reference evapotranspiration (ET_o) values of day i, calculated by the Penman-Monteith method and the other methods (Blaney-Criddle or Hargreaves-Samani) respectively, $\bar{E}T_{PM}$ is the average over the data period while n is the sample size. The smaller the indices of MAE, MBE and RMSE, the better the agreement between ET_o computed by other methods and ET_o computed by the Penman-Monteith method. The values of CE range from -∞ to 1, with CE = 1 being the optimal value, values between 0 and 1 indicate acceptable levels of performance whereas values less than 0 indicate unacceptable performance.

2.4. Global Sensitive Analysis

A global sensitivity analysis was conducted for all three ET_o estimation approaches to determine the influence that measured parameters had on simulated ET_o. Crystal Ball (Oracle Inc., Redwood City, CA), based on the Sobol method [51], was used to quantify the contribution of each input parameter to the change of the simulated results. The parameter interactions were considered in this approach. A Monte Carlo simulation [52] was implemented to provide natural random variation of each parameter within their observed ranges. In the simulation, each parameter was subsampled 10,000 times, represented by their mean values and standard deviations across all the observations under an assumed normal distribution [53]. After analyzing the pattern of these 10,000 trials of data derived from Monte Carlo simulation, a distribution of predicted ET_o was shown. In this study, the mean standard deviation of predicted ET_o was 2.13 mm, 2.81 mm, and 2.27 mm for the Penman-Monteith, Blaney-Criddle and Hargreaves-Samani methods, respectively. Finally, the software produced the contribution of each input parameter to the variability of the predicted ET_o. The greater the percentage, the more sensitive a model output variable is to that particular parameter.

 doi:10.20944/preprints202407.0673.v1

3. Results

3.1. Temporal Variation in Soil Water Content (SWC) and Deep Percolation (DP)

The significant fluctuations in soil moisture for each depth were caused by each irrigation event (Figure 3). The average SWC at 15, 30, 50 and 80 cm were, respectively, 33.2±0.4%, 36.4±0.2%, 39.8±0.1%, and 39.9±0.4 % for the 2021-22 growing season, and 34.0±0.3%, 35.4±0.2%, 35.8±0.04% and 37.5±0.1% for the 2022-23 growing season. The average soil moisture depletion (ΔSWC) between before and after irrigation at 15, 30, 50, and 80 cm were 13.8%, 5.3%, 2.4%, and 6.4% throughout the 2021-22 season, and 15.0%, 11.8%, 1.7% and 4.7% throughout the 2022-23 season, respectively, the high values of depletion at 80 cm indicated that deep percolation cannot be negligible in this study. In our study, an additional irrigation event was applied in the 2021-22 growing season for the 2022-23 growing season where intense precipitation occurred in October (Figure 3). The DP for each irrigation event ranged from 9.8% to 39.7% of the irrigation amount throughout the 2021-22 season, and from 17.8% to 33.0% throughout the 2022-23 season.

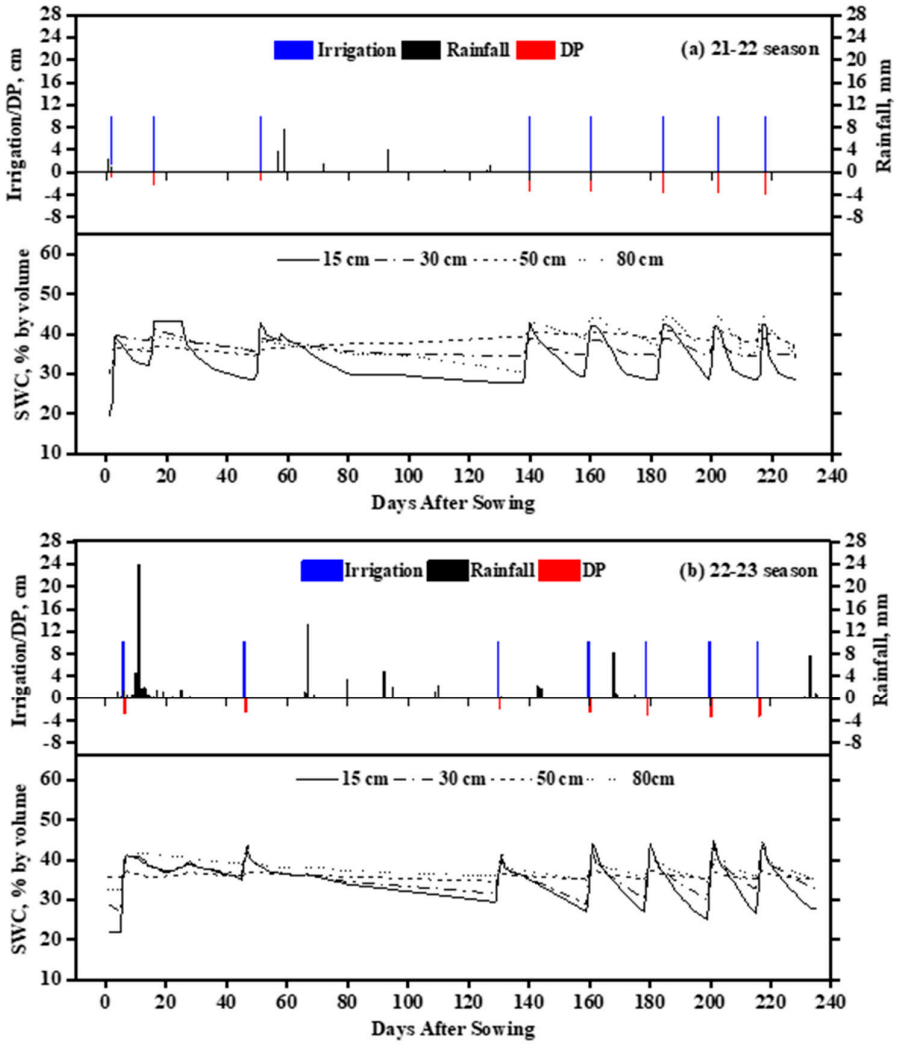

Figure 3. Irrigation amount, rainfall, deep percolation (DP), and volumetric soil water content (SWC) of the root zone in the experimental winter wheat field in New Mexico during the 2021-2022 (a), 2022-2023(b) growing seasons.

 doi:10.20944/preprints202407.0673.v1

3.2. Reference Evapotranspiration Using the Three Contrasting Methods

The total ET_c during the whole growing season was 564.2 mm and 548.6 mm for 2021-22 and 2022-23, respectively. The ET_o computed by the Penman-Monteith, Blaney-Criddle and Hargreaves-Samani methods were 867.0 mm and 785.6 mm, 1015.0 mm and 947.0 mm, 856.2 mm and 800.1 mm, respectively over the two periods of winter wheat growth stage (Figure 4). Compared to the Penman-Monteith method, Blaney-Criddle overestimated ET_o by 17.1% and 20.5%, respectively in 2021-22 and 2022-23 season, while Hargreaves-Samani underestimated ET_o by 1.2% in 2021-22 season and overestimated ET_o by 1.8% in the 2022-23 season. The goodness of fit indicators confirmed the better performance of the Hargreaves-Samani method, which had higher CE, and smaller MBE, MAE, and RMSE for both growing seasons (Table 4).

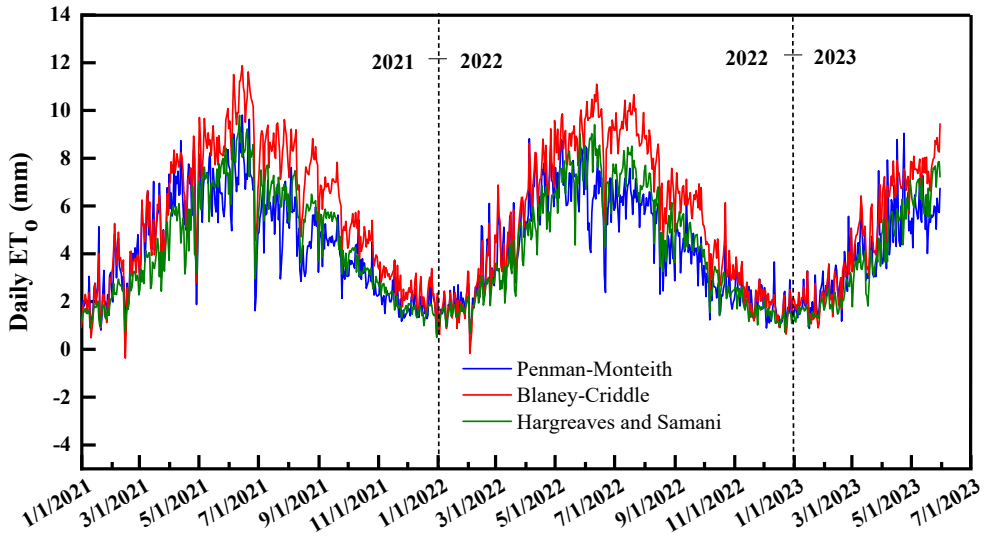

Figure 4. Daily reference evapotranspiration (ET_o, mm) under contrasting ET estimation methods (Penman-Monteith, Blaney-Criddle, and Hargreaves-Samani) over two growing seasons of winter wheat in New Mexico from 2021 to 2023.

Table 4. Goodness of fit indicators for the comparison between the Blaney-Criddle and Hargreaves-Samani methods against the Penman-Monteith equation to calculate reference evapotranspiration. CE: Nash-Sutcliffe model efficiency coefficient, MBE: the mean bias error, MAE: the mean absolute error, and RMSE: the root mean square error.

Growing season	Method	CE (%)	MBE (mm)	MAE (mm)	RMSE (mm)
2021-2022	Blaney-Criddle	79.8	0.59	0.73	0.92
	Hargreaves	80.2	-0.07	0.67	0.91
2022-2023	Blaney-Criddle	54.9	0.61	0.85	1.13
	Hargreaves	67.9	0.03	0.70	0.96

3.3. Input Parameters' Assessment for the Three ET_o Estimation Methods

The results of the global sensitivity analysis are displayed in Figure 5, which reported the sensitivity percentage of input meteorological variables based on crystal ball analysis for three ET_o estimation methods. For Penman-Monteith, wind speed and maximum temperature were the driving factors affecting ET_o the most, with sensitivity percentages of 70.9% and 21.9%, respectively. Solar radiation ranked third, with a sensitivity percentage of 4.0%.

Regarding the two temperature-based methods, mean temperature, percent sun, and minimum relative humidity were the first three factors influencing the simulated ET_o based on Blaney-Criddle,

 doi:10.20944/preprints202407.0673.v1

their sensitivity percentages were 76.9%, 15.4%, and 6.6%, respectively. Mean temperature, Julian day, and minimum temperature, with sensitivity percentages of 48.9%, 26.3%, and 15.9%, respectively, affected the simulated ET_o based on Hargreaves-Samani.

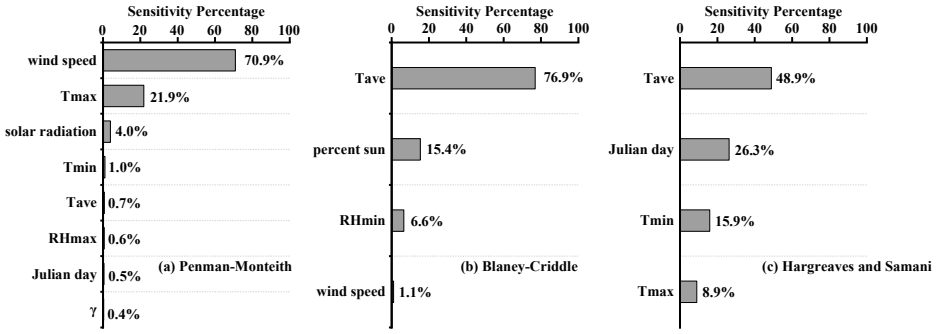

Figure 5. Sensitivity percentages of input meteorological variables based on crystal ball analysis, for three ET_o estimation methods: (a) Penman-Monteith; (b) Blaney-Criddle; (c) Hargreaves and Samani. Tave, T_{max}, and T_{min} are daily mean, maximum, and minimum temperature (℃), respectively, RH_{max} and RH_{min} are daily maximum and minimum relative humidity (%), γ is the psychrometric constant (kPa ℃$^{-1}$).

3.4. Crop Coefficients

Crop coefficients (K_c) of two seasons were consistent with the general trend that K_c values were lower in the early-season stages and late-season stages toward harvest, but gradually increased in the mid-season stages in spring (Figure 6). The K_c exhibited a single-peak curve throughout the 2021-22 growing season, average K_c values were 0.50, 0.46 and 0.47 for the early-season, 1.25, 1.12 and 1.41 for the mid-season, and 0.53, 0.48 and 0.59 for the late season according to the Penman-Monteith, Blaney-Criddle, and Hargreaves-Samani methods, respectively. However, during the 2022-23 season, K_c showed a bimodal curve over time; average K_c values were 0.58, 0.56, and 0.57 for the early-season, 0.90, 0.84 and 0.99 for the mid-season, 0.54, 0.43 and 0.53 for the late-season according to the Penman-Monteith, Blaney-Criddle, and Hargreaves-Samani methods, respectively.

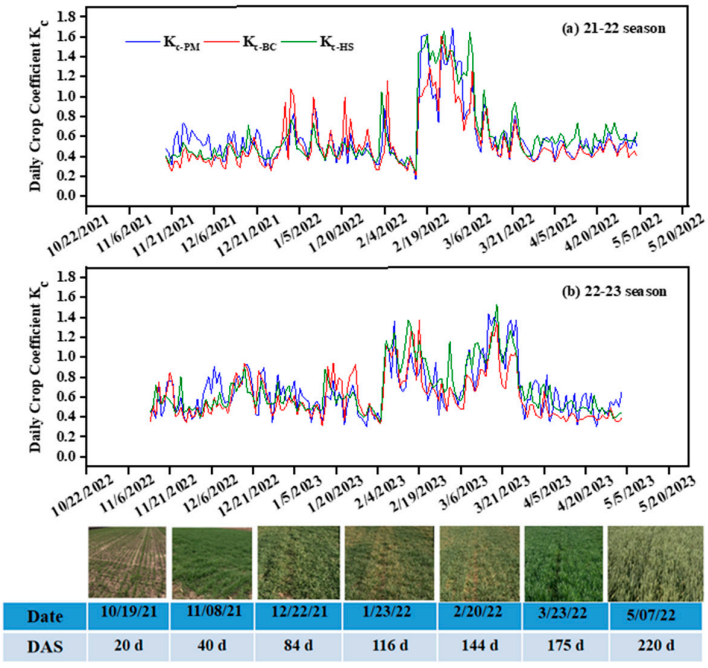

 doi:10.20944/preprints202407.0673.v1

Figure 6. Daily crop coefficients (K_c) of winter wheat calculated by three ET_o estimation methods during two growing seasons in New Mexico. Digital photographs were taken on 10/19, 11/08, 12/22, 2021, and 1/23, 2/20, 3/23, and 05/07, 2022 through the 2021-2022 growing season, the corresponding days after sowing (DAS) were listed.

4. Discussion

ET_o represents the primary weather-induced influences on the evapotranspiration rate of the grass reference crop [17]. The Penman-Monteith equation was found to be the most precise method to estimate ET_o under a wide range of climatic conditions [16,22–24,54,55], whereas the Hargreaves-Samani and Blaney-Criddle equations are two temperature-based and alternative widely used approaches that produce acceptable estimations under diverse climates using limited meteorological data [56,57]. Among which Hargreaves-Samani was reported to perform poorly in extremely windy and humid conditions [58]. Our study found both Hargreaves-Samani and Blaney-Criddle methods overestimated ET_o when compared to the Penman-Monteith method in the Lower Rio Grande Valley of southern New Mexico, Hafeez et al. [36] also found that Blaney-Criddle and Hargreaves-Samani overestimated ET_o by 23.78% and 37.93% compared to the Penman-Monteith method for a humid subtropical climate. Valipour [59] compared 11 temperature-based models with the PM method and found that the modified Hargreaves-Samani method estimated ET_o better than other models in most provinces of Iran. Our results also indicated that the Hargreaves-Samani method performed better than the Blaney-Criddle method with higher CE, and smaller MBE, MAE, RMSE for both growing seasons (Table 4 and Figure 4). This finding might be explained by the results of global sensitivity analysis, the sensitivity percentage of average temperature for Blaney-Criddle was 76.9%, much higher than that of 48.9% for Hargreaves-Samani (Figure 5), given that the ET_o estimated by Blaney Criddle is more fluctuant and less accurate than ET_o estimated by Hargreaves-Samani during growing season, especially in arid area such as Lower Rio Grande Valley where the monthly average temperature is over 20℃ from May to September and the seasonal variation is large (Figure 2).

The crop coefficient (K_c), defined as the ratio of ET_c/ET_o, represents specific crop characteristics. It is affected by crop varieties, irrigation management, and environmental conditions but varies little with climate change [60]. Various authors reported K_c values for winter wheat in various locations and irrigation methods. Some reported that the K_c value of winter wheat in monoculture ranges between 0.26-0.80, 0.91-1.44, 0.27-0.98 at initial, mid, and late growth stages, respectively in Northern China [43,61–63], while the K_c values for initial, mid-, and end-season of winter wheat were, respectively, 0.77, 1.35 and 0.26 in Southwest Iran [57]. Site-specific measurements and observations of crop growth are expected to be more accurate in estimating crop water use and optimizing irrigation scheduling [64]. To the best of our knowledge, no precise information on K_c is reported in southern New Mexico. Our study presented the daily values of K_c from equations (Figure 6), which is very useful towards efficient management of irrigation water [65]. The two-year average K_c values were 0.54, 0.51, and 0.52 for the early-season, 1.1, 1.0 and 1.2 for the mid-season, 0.54, 0.46 and 0.56 for the late-season crop growth stages according to the Penman-Monteith, Blaney-Criddle, and Hargreaves-Samani method, respectively (Figure 6). In comparison with the K_c values from Uvalde Texas [21], our values are similar at early and mid-growth stages to those of 0.53 and 1.15 and slightly larger at late growth stage than that of 0.40. Howell et al. [50] reported K_c values for winter wheat at Bushland, Texas High Plains, where the peak value of K_c was 0.94, and initial and late K_c were 0.29 and 0.30, respectively.

The K_c curve represents the variations of K_c over the crop growing season [20], it showed unimodal and bimodal trends, respectively for the 2021-22 and the 2022-23 seasons in this study (Figure 6). The K_c values for mid-season first decreased, then gradually increased during the period from February 16 to March 8 in the 22-23 season, which resulted from much lower calculated ET_c during this period than that of the 21-22 season. This finding might be explained by the reason that the accumulated growing degree days (GDD) during this period ranged from 513.0 ℃ to 705.8 ℃ in the 22-23 season, which was lower than that of the 21-22 season (543.1 ℃ to 725.7 ℃) (Figure 7), consequently giving the lower ET_c for the period from February 16 to March 8 in 22-23 seasons.

 doi:10.20944/preprints202407.0673.v1

Moreover, the irrigation date after the winter season in 22-23 season was 2/6/2023, which was 10 days in advance compared to that in the 21-22 season (2/16/2022), this practice also exacerbated the decrease in ET_c. This phenomenon indicated that irrigation time is critical in establishment of irrigation regimes by meeting the specific water needs of individual crops and ensuring optimal water-saving [66]. In our future study, more detailed crop growth datasets will be observed in leaf area, crop height, leaf age and conditions, and fraction of ground covered by the vegetation, we will further calculate K_c with FAO56 methods based on its theoretical background and compare the K_c values with those calculated by ratio of ET_c to ET_o.

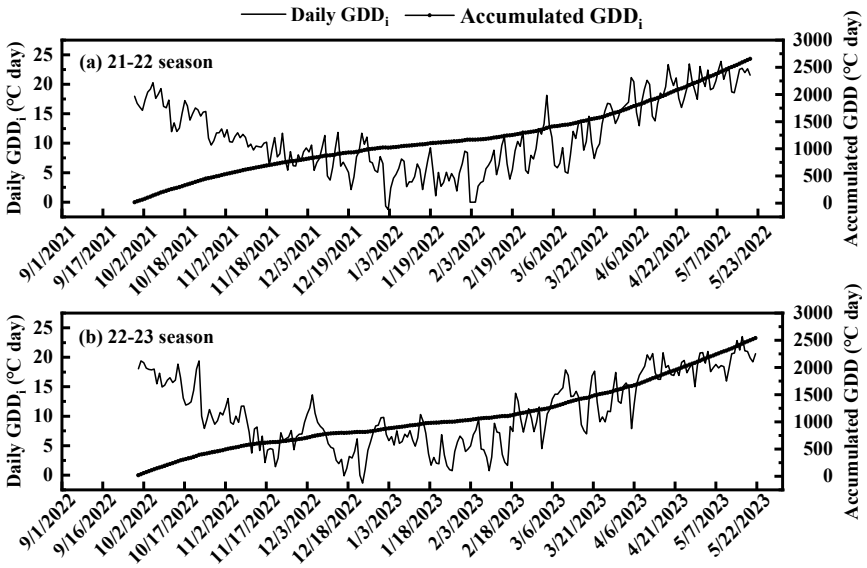

Figure 7. Daily and accumulated growing degree days (GDD) during the 2021-22 (a) and 2022-23 (b) growing seasons of experimental winter wheat in New Mexico.

5. Conclusions

The crop coefficient (K_c) of flood-irrigated winter wheat was assessed under three reference evapotranspiration (ET_o) estimation methods in the Lower Rio Grande Valley of southern New Mexico. The total crop evapotranspiration (ET_c) during the whole growth stage was 556.4 mm on average for flood-irrigated winter wheat devoted to forage in this study area. Both Blaney-Criddle and Hargreaves-Samani equations overestimated ET_o, when Penman-Monteith was considered as a reference, the global sensitivity analysis showed that average temperature accounted for 76.9%, of sensitivity for the Blaney-Criddle method, which was much higher than that for Hargreaves-Samani (48.9%). This suggests that the Hargreaves-Samani equation could be a reliable alternative tool to predict ET_o when a lower number of meteorological variables are available in this area. The two-year average crop coefficient (K_c) values at the initial, mid, and late growth stage were 0.54, 1.1, and 0.54 for the Penman-Monteith method, 0.51, 1.0 and 0.46 for the Blaney-Criddle method, and 0.52, 1.2 and 0.56 for the Hargreaves-Samani method. The irrigation should be applied based on the growth-stage-specific K_c to improve water use efficiency.

Author Contributions: Conceptualization, H.Y., and M.S.; methodology, H.Y., and Y.Y.; software, H.Y, and Y.Y.; validation, H.Y., Y.Y., A.G., and M.S.; formal analysis, H.Y.; investigation, H.Y., and A.G.; resources, H.Y.; data curation, H.Y.; writing—original draft preparation, H.Y.; writing—review and editing, H.Y.; visualization, H.Y.; supervision, M.S.; project administration, M.S.; funding acquisition, M.S. All authors have read and agreed to the published version of the manuscript.

Funding: This project was supported by the New Mexico Department of Agriculture and Interstate Stream Commission for funding.

Data Availability Statement: The data presented in this study are available on request due to ongoing project research.

Acknowledgments: The authors thank NIFA, NMSU Agricultural Experiment Station, and Nakayama Professorship endowment for support.

Conflicts of Interest: The authors declare no conflict of interest.

References

1. Franch, B.; Vermote, E.F.; Becker-Reshef, I.; Claverie, M.; Huang, J.; Zhang, J.; Justice, C.; Sobrino, J.A. Improving the timeliness of winter wheat production forecast in the United States of America, Ukraine and China using MODIS data and NCRA growing degree day information. Remote Sens. of Environ. 2015, 161, 131-148. https://doi.org/10.1016/j.rse.2015.02.014.
2. Wu, X.C.; Xiao, X.M.; Steiner, J.; Yang, Z.W.; Qin, Y.W.; Wang, J. Spatiotemporal changes of winter wheat planted and harvested areas, photosynthesis and grain production in the contiguous United States from 2008-2018. Remote Sens. 2021, 13, 1735. https://doi.org/10.3390/rs13091735.
3. Maulana, F.; Kim, K.S.; Anderson, J.D.; Sorrells, M.E.; Butler, T.J.; Liu, S.Y.; Baenziger, P.S.; Byrne, P.F.; Ma, X.F. Genomic selection of forage quality traits in winter wheat. Crop Sci. 2019, 59, 2473-2483. http://creativecommons.org/licenses/by-nc-nd/4.0/.
4. United States Department of Agriculture, National Agricultural Statistics Service. News Release, January 12, 2021, New Mexico Field Office. https://www.nass.usda.gov/Statistics_by_State/New_Mexico/Publications/News_Releases/2021/NM-Crop-Production-01122021.pdf.
5. United States Department of Agriculture, National Agricultural Statistics Service. New Mexico crop progress, May 31, 2022, New Mexico Field Office. https://www.nass.usda.gov/Statistics_by_State/New_Mexico/Publications/Crop_Progress_%26_Condition/2022/NM-Crop-Progress-05222022.pdf.
6. Tapley, M.; Ortiz, B.V.; Santen, E.V.; Balkcom, K.S.; Mask, P.; Weaver, D.B. Location, seeding date, and variety interactions on winter wheat yield in Southeastern United States. Agron. J. 2013, 105(2), 509-518. http://doi.org/10.2134/AGRONJ2012.0379.
7. Vitale, J.; Adam, B.; Vitale, P. Economics of wheat breeding strategies: focusing on Oklahoma Hard Red winter wheat. Agron. 2020, 10, 238. https://doi.org/10.3390/agronomy10020238.
8. Deb, S.K.; Shukla, M.K.; Sharma, P.; Mexal, J.G. Soil water depletion in irrigated mature peacans under contrasting soil textures for arid Southern New Mexico. Irrig. Sci. 2013, 31, 69-85. http://doi.org/10.1007/s00271-011-0293-1.
9. Office of the State Engineer, State of New Mexico. Lower Rio Grande Regional Water Plan 2017. https://www.ose.state.nm.us/Planning/documents/Reg11_LowerRioGrande RegionalWaterPlan2017pdf.
10. López-Urrea, R.; Sánchez, J.M.; de la Cruz, F.; González-Piqueras, J.; Chávez, J.L. Evapotranspiration and crop coefficients from lysimeter measurements for sprinkler irrigated canola. Agric. Water Manag. 2020, 239, 106260. https://doi.org/10.1016/j.agwat.2020.106260.
11. Er-Raki, S.; Ezzahar, J.; Merlin, O.; Amazirh, A.; Hssaine, B.A.; Kharrou, M.H.; Khabba, S.; Chehbouni, A. Performance of the HYDRUS-1D model for water balance components assessment of irrigated winter wheat under different water managements in semi-arid region of Morocco. Agric. Water Manag. 2021, 244, 106546. https://doi.org/10.1016/j.agwat.2020.106546.
12. Rashid Niaghi, A.; Jia, X. New approach to improve the soil water balance method for evapotranspiration estimation. Water. 2019, 11 (12), 2478. https://doi.org/10.3390/w11122478.
13. Pereira, L.S.; Paredes, P.; Jovanovic, N. Soil water balance models for determining crop water and irrigation requirements and irrigation scheduling focusing on the FAO56 method and the dual Kc approach. Agric. Water Manag. 2020, 241, 106357. https://doi.org/10.1016/j.agwat.2020.106357.
14. Rafi, Z.; Merlin, O.; Le Dantec, V.; Khabba, S.; Mordelet, P.; Er-Raki, S.; Ferrer, F. Partitioning evapotranspiration of a drip-irrigated wheat crop: Inter-comparing eddy covariance-, sap flow-, lysimeter- and FAO-based methods. Agric. For. Meteorol. 2019, 265, 310-326. https://doi.org/10.1016/j.agrformet.2018.11.031.
15. Chen, X.; Su, Z.; Ma, Y.; Middleton, E.M. Optimization of a remote sensing energy balance method over different canopy applied at global scale. Agric. For. Meteorol. 2019, 279, 107633. https://doi.org/10.1016/j.agrformet.2019.107633.

16. Allen, R.G.; Pereira, L.S.; Howell, T.A.; Jensen, M.E. Evapotranspiration information reporting: I. Factors governing measurement accuracy. Agric. Water Manag. 2011, 98, 899-920. https://doi.org/10.1016/j.agwat.2010.12.015.
17. Pereira, L.S.; Paredes, P.; López-Urrea, R.; Hunsaker, D.J.; Mota, M.; Mohammadi Shad, Z. Standard single and basal crop coefficients for vegetable crops, an update of FAO56 crop water requirements approach. Agric. Water Manag. 2021, 243, 106196. https://doi.org/10.1016/j.agwat.2020.106196.
18. Mokhtari, A.; Noory, H.; Vazifedoust, M.; Bahrami, M. Estimating net irrigation requirement of winter wheat using model- and satellite-based single and basal crop coefficients. Agric. Water Manag. 2018, 208, 95-106. https://doi.org/10.1016/j.agwat.2018.06.013.
19. Tegos, A.; Malamos, N.; Koutsoyiannis, D. A parsimonious regional parametric evapotranspiration model based on a simplification of the Penman-Monteith formula. J. Hydrol. 2015, 524, 708-717. https://doi.org/10.1016/j.jhydrol.2015.03.024.
20. Allen, R.G.; Pereira, L.S.; Raes, D.; Smith, M. Crop evapotranspiration-Guidelines for computing crop water requirements-FAO Irrigation and drainage paper 56, FAO, Rome, vol. 300, 1998, p. D05109.
21. Ko, J.H.; Piccinni, G.; Marek, T.; Howell, T. Determination of growth-stage-specific crop coefficients (Kc) of cotton and wheat. Agric. Water Manag. 2009, 96, 1691-1697. https://doi.org/10.1016/j.agwat.2009.06.023.
22. Ghamarnia, H.; Mousabeygi, F.; Amiri, S.; Amirkhani, D. Evaluation of a few evapotranspiration models using lysimeteric measurements in a semi-arid climate region. Int. J. Plant &Soil Sci. 2015, 5(2), 100-109. http://doi.org/10.9734/IJPSS/2015/14320.
23. Tahashildar, M.; Bora, P.K.; Ray, L.I.P.; Thakuria, D. Comparison of different reference evapotranspiration (ETo) models and determination of crop-coefficients of french bean (Phesiolus vulgaris) in mid hill region of Meghalaya. J. Agrometeorol. 2017, 19(3), 233-237.
24. Djaman, K.; O'Neill, M.; Diop, l.; Bodian, A.; Allen, S.; Koudahe, K.; Lombard, K. Evaluation of the Penman-Monteith and other 34 reference evapotranspiration equations under limited data in a semiarid dry climate. Theor. Appl. Climatol. 2019, 137, 729-743. http://doi.org/10.1007/s00704-018-2624-0.
25. Droogers, P.; Allen, R.G. Estimating reference evapotranspiration under inaccurate data conditions. Irrig. Drain. Sys. 2002, 16 (1), 33-45. https://doi.org/10.1023/A:1015508322413.
26. Jabloun, M.D.; Sahli, A. Evaluation of FAO-56 methodology for estimating reference evapotranspiration using limited climatic data: application to Tunisia. Agric. Water Manag. 2008, 95 (6), 707-715. https://doi.org/10.1016/j.agwat.2008.01.009.
27. Almorox, J.; Quej, V.H.; Martí, P. Global performance ranking of temperature-based approaches for evapotranspiration estimation considering Köppen climate classes. J. Hydrol. 2015, 528, 514-522. https://doi.org/10.1016/j.jhydrol.2015.06.057.
28. Samani, Z. Estimating solar radiation and evapotranspiration using minimum climatological data. J. Irrig. Drain. Eng. 2000, 126 (4), 265-267. https://doi.org/10.1061/(ASCE)0733-9437(2000)126:4(265).
29. Hargreaves, G.H.; Samani, Z.A. Reference crop evapotranspiration from temperature. Appl. Eng. Agric. 1985, vol. 1, pp. 96-99. http://doi.org/10.13031/2013.26773.
30. Doorenbos, J.; W.O. Pruitt. Guidelines for predicting crop water requirements. Irrigation And Drainage. Paper No. 24, 2nd edition, Food and Agricultural Organization of the United Nations, Rome, Italy, 1977, 156 pp.
31. Blaney, H.F.; Morin, K.V. Evaporation and consumptive water use of water, empirical formulae. Pt. 1. Am. Geophys. Union Trans. 1942a, p76-83.
32. Blaney, H.F.; Ewing, P.A.; Morin, K.V; Criddle, W.D. Consumptive waster use and requirements. The Pecos river joint investigation, reports of the participating agencies. National Resources Planning Board. 1942b, p170-230.
33. Shahidian, S.; Serralheiro, R.P.; Serrano, J.; Teixeira, J.L. Parametric calibration of the Hargreaves-Samani equation for use at new locations. Hydrol. Process. 2013, 27, 605-616. http://doi.org/10.1002/hyp.9277.
34. Awal, R.; Habibi, H.; Fares, A.; Deb, S. Estimating reference crop evapotranspiration under limited climate data in West Texas. J. Hydrol. Reg. Stud. 2020, 28, 100677. https://doi.org/10.1016/j.ejrh.2020.100677.
35. Thongkao, S.; Ditthafit, P.; Pinthong, S.; Salaeh, N.; Elkhrachy, I.; Linh, N.T.T.; Pham, Q.B. Estimating FAO Blaney-Criddle b-factor using soft computing models. Atm. 2022, 13, 1536. https://doi.org/10.3390/atmos13101536.

36. Hafeez, M.; Ahmad Chatha, Z.; Akhtar Khan, A.; Bakhsh, A.; Basit, A.; Tahira, F. Estimating reference evapotranspiration by Hargreaves and Blaney-Criddle methods in humid subtropical conditions. Curr. Res. Agric. Sci. 2020, 7(1), 15-22. https://orcid.org/0000-0002-3262-7014.
37. Gee, G.W.; Bauder, J.W. Particle-size Analysis, in: Klute, A. (Ed.), SSSA Book Series. Soil Science Society of America, American Society of Agronomy, Madison, WI, USA, 2018, pp. 383-411. https://doi.org/10.2136/sssabookser5.1.2ed.c15.
38. Blake, G.R.; Hartge, K.H. Bulk density. Methods Soil Anal. 1986, 363-375.
39. Klute, A.; Dirkson, C. Hydraulic conductivity and diffusivity: Laboratory Methods. In A. Klute (Ed.) "Methods of soil analysis, Part I." ASA Monograph No.9. Madison, WI, 1986, pp. 687-734.
40. Klute, A. Water retention: laboratory methods. In A. Klute (Ed.) "Methods of soil analysis. Part 1." 2nd ed. Agron. Monogr.9. ASA. Madison, WI, 1986, pp. 635-661.
41. Kargas, G.; Soulis, K.X. Performance evaluation of a recently developed soil water content, dielectric permittivity, and bulk electrical conductivity electromagnetic sensor. Agric. Water Manag. 2019, 213, 568-579. https://doi.org/10.1016/j.agwat.2018.11.002.
42. Evett, S.R.; Tolk, J.A.; Howell, T.A. Soil profile water content determination: sensor accuracy, axial response, calibration, temperature dependence, and precision. Vadose Zone J. 2006, 5 (3), 894-907. https://doi.org/10.2136/vzj2005.0149.
43. Kang, S.Z.; Gu, B.J.; Du, T.S.; Zhang, J.H. Crop coefficient and ratio of transpiration to evapotranspiration of winter wheat and maize in a semi-humid region. Agric. Water Manag. 2003, 59, 239-254. https://doi.org/10.1016/S0378-3774(02)00150-6.
44. Gao, X.Y.; Tang, P.C.; Wang, Z.W.; Yao, Y.T.; Qu, Z.Y.; Yang, W.; Du, B. Crop coefficient of Sunflowers under drip irrigation with plastic film in different hydrological years in the Hetao irrigation district. Water. 2024, 16, 235. https://doi.org/10.3390/w16020235.
45. Silva Junior, A.C.d.; Souza, P.J.d.O.P.d.; Sousa, D.d.P.; Martorano, L.G.; Silva, C.M.d.; Silva, C.M.d.; Nunes, H.G.G.C.; Lima, M.J.A.d.; Sousa, A.M.L.d.; Pinto, J.V.d.N.; Ruivo, M.d.L.P.; Alves, J.D.N. Energy balance, water demand, and crop coefficient of acid lime in the Oriental Amazon. Water. 2023, 15, 1239. https://doi.org/10.3390/w15061239.
46. Jensen, M.E.; Burman, R.D.; Allen, R.G. Evapotranspiration and irrigation water requirements. ASCE Manuals and Reports on Engineering Practice. 1990, No. 70, p. 332.
47. Allen, R.G.; Smith, M.; Pereira, L.S. An update for the definition of reference evapotranspiration. ICID Bull, 1994, 43, 1-34.
48. United States Department of Agriculture, Soil Conservation Service. Irrigation water requirement. Part 623 National Engineering Handbook. Chapter 2. 1993, pp56-60.
49. Deb, S.K.; Shukla, M.K.; Mexal, J.G. Simulating deep percolation in flood-irrigated mature pecan orchards with RZWQM2. Trans. ASABE. 2012, 55(6), 2089-2100. http://doi.org/10.13031/2013.42501.
50. Howell, T.A.; Steiner, J.L.; Schneider, A.D.; Evett, S.R. Evapotranspiration of irrigated winter wheat southern high plains. Trans. ASABE. 1995, 38(3), 745-759. http://doi.org/10.13031/2013.27888.
51. Zhang, X.Y.; Trame, M.; Lesko, L.; Schmidt, S. Sobol sensitivity analysis: a tool to guide the development and evaluation of systems pharmacology models. CPT: Pharmacometrics & Systems Pharmacology, 2015, 4, 69-79. https://doi.org/10.1002/psp4.6.
52. Bhat, A.; Kumar, A. Application of the Crystal Ball software for uncertainty and sensitivity analyses for predicted concentration and risk levels. Environ. Prog. 2008, 27, 289-294. https://doi.org/10.1002/ep.10308.
53. Yuan, Y.S.; Wang, L.X.; Wang, H.L.; Lin, W.Q.; Jiao, W.Z.; Du, T.S. A modified isotope-based method for potential high-frequency evapotranspiration partitioning. Adv. Water Resour. 2022, 160, 104103. https://doi.org/10.1016/j.advwatres.2021. 104103.
54. López-Urrea, R.; Martín de Santa Olalla, F.; Fabeiro, C.; Moratalla, A. Testing evapotranspiration equations using lysimeter observations in a semiarid climate. Agric. Water Manag. 2006, 85, 15-26. https://doi.org/10.1016/j.agwat.2006.03.014.
55. Martel, M.; Glenn, A.; Wilson, H.; Kröbel, R. Simulation of actual evapotranspiration from agricultural landscapes in the Canadian Prairies. J. Hydrol. Reg. Stud. 2018, 15, 105-118. https://doi.org/10.1016/j.ejrh.2017.11.010.
56. Sammis, T.W.; Wang, J.M.; Miller, D.R. The transition of the Blaney-Criddle formula to the Penman-Monteith equation in the western United States. J. Serv. Climatol. 2011, 5(1), 1-11. http://doi.org/10.46275/joasc.2011.02.001.

57. Shahrokhnia, M.H.; Sepaskhah, A.R. Single and dual crop coefficients and crop evapotranspiration for wheat and maize in a semi-arid region. Theor. Appl. Climatol. 2013, 114, 495-510. https://doi.org/10.1007/s00704-013-0848-6.
58. Xu, C.Y.; Singh, V.P. Cross comparison of empirical equations for calculating potential evapotranspiration with data from Switzerland. Water Resour. Manag. 2002, 16, 197-219. https://doi.org/10.1023/A:1020282515975.
59. Valipour, M. Temperature analysis of reference evapotranspiration models. Meteorol. Appl. 2015, 22, 385-394. http://doi.org/10.1002/met.1465.
60. Zhang, B.Z.; Liu, Y.; Xu, D.; Zhao, N.N.; Lei, B.; Rosa, R.D.; Paredes, P.; Paço, T.A.; Pereira, L.S. The dual crop coefficient approach to estimate and partitioning evapotranspiration of the winter wheat-summer maize crop sequence in North China Plain. Irrig. Sci. 2013, 31, 1303-1316. https://doi.org/10.1007/s00271-013-0405-1.
61. Gao, Y.; Duan, A.W.; Sun, J.S.; Li, F.S.; Liu, Z.G.; Liu, H.; Liu, Z.D. Crop coefficient and water-use efficiency of winter wheat/spring maize strip intercropping. Field Crops Res. 2009, 111, 65-73. https://doi.org/10.1016/j.fcr.2008.10.007.
62. Gao, Y.; Yang, L.L.; Shen, X.J.; Li, X.Q.; Sun, J.S.; Duan, A.W.; Wu, L.S. Winter wheat with subsurface drip irrigation (SDI): Crop coefficients, water-use estimates, and effects of SDI on grain yield and water use efficiency. Agric. Water Manag. 2014, 146, 1-10. https://doi.org/10.1016/j.agwat.2014.07.010.
63. Wang, J.D.; Zhang, Y.Q.; Gong, S.H.; Xu, D.; Juan, S.; Zhao, Y.F. Evapotranspiration, crop coefficient and yield for drip-irrigated winter wheat with straw mulching in North China Plain. Field Crops Res. 2018, 217, 218-228. https://doi.org/10.1016/j.fcr.2017.05.010.
64. Drerup, P.; Brueck, H.; Scherer, H.W. Evapotranspiration of winter wheat estimated with the FAO 56 approach and NDVI measurements in a temperature-humid climate of NW Europe. Agric. Water Manag. 2017, 192, 180-188. http://dx.doi.org/10.1016/j.agwat.2017.07.010.
65. Dingre, S.K.; Gorantiwar, S.D. Determination of the water requirement and crop coefficient values of sugarcane by field water balance method in semiarid region. Agric. Water Manag. 2020, 232, 106042. https://doi.org/10.1016/j.agwat.2020.106042.
66. Abioye, E.A.; Abidin, M.S.Z.; Mahmud, M.S.A.; Buyamin, S.; Ishak, M.H.I.; Rahman, M.K.I.A.; Otuoze, A.O.; Onotu, P.; Ramli, M.S.A. A review on monitoring and advanced control strategies for precision irrigation. Comput. Electron. Agric. 2020, 173, 105441.https://doi.org/10.1016/j.compag.2020.105441.